GEOPHYSICAL RESEARCH LETTERS, VOL. 22, NO. 22, PAGES 3099-3102, NOVEMBER 15, 1995

Spherical-spline parameterization of three-dimensional Earth models

Zheng Wang[1] and F. A. Dahlen

Department of Geological and Geophysical Sciences, Princeton University, Princeton, New Jersey

Abstract. We propose a spherical surface-spline method that parameterizes a two-dimensional model on a sphere in terms of a local cubic B-spline basis on a triangular grid of knots with approximately equal inter-knot spacing. Numerical results show that such a parameterization can represent a model on a sphere with an accuracy equal to that of the spherical-harmonic parameterization of the corresponding nominal degree. Furthermore, it significantly reduces the computational time needed to calculate surface-wave synthetic seismograms on a laterally heterogeneous Earth, and makes it feasible to apply JWKB theory to surface-wave inversion studies.

Introduction

Imaging the interior of the Earth has been a major task in seismology for several decades. Utilizing high-quality digital seismic data, seismologists have made rapid progress in determining the laterally varying structure of the mantle [*Masters et al.*, 1982; *Woodhouse and Dziewonski,* 1984; *Woodhouse and Wong,* 1986; *Zhang and Tanimoto,* 1992; *Su et al.*, 1994]. Most studies have made use of a great-circle approximation method [*Woodhouse and Dziewonski,* 1984; *Woodhouse and Wong,* 1986; *Um and Dahlen,* 1992], which is valid for small and smooth variations, to linearize the inverse problem. *Wang and Dahlen* [1994] have concluded that this first-order perturbation theory could result in large discrepancies compared to full surface-wave JWKB theory even on a relatively smooth model such as S12_WM13 [*Su et al.*, 1994]. They suggest that the full theory [*Tromp and Dahlen,* 1992] should be used in surface-wave inversion studies in order to resolve higher-degree variations in the mantle.

In the past, the JWKB method has been implemented on Earth models that are parameterized in terms of spherical harmonics. Such an expansion, however, necessitates a significant increase in computational time with increasing angular degree, on the one hand, and is impractical in regional studies limited to just a portion of the globe, on the other hand. To remedy these limitations, a parameterization method that partitions the earth's surface into a set of equal-area blocks and assigns each block a constant velocity has been employed in some studies [*Clayton and Comer,* 1983; *Zhang and Tanimoto,* 1992]. Such a block parameterization can be applied to regional studies; however, because of its discontinuity from one block to another, it cannot be used to perform dynamic as well as kinematic ray tracing, which is essential to the surface-wave JWKB method.

In this paper, we present a spherical surface-spline method that parameterizes the laterally variable phase velocity of a Love or Rayleigh surface wave in terms of cubic B-splines centered upon a discrete number of geographical knots. The resulting model has continuous zeroth, first and second derivatives everywhere in the surface spherical coordinates θ, ϕ. A triangular tessellation technique is used to configure the knots upon the earth's surface; this method guarantees that the geodesic distance between neighbouring grid points exhibits less than 8 percent variation, and allows arbitrary grid density. A linear interpolation scheme based upon a spherical tessellation grid has been applied to geomagnetic problem by Constable *et al.* [1993].

Spherical Tessellation

It is well known that a spherical surface can not be partitioned into spherical rectangles of equal area, as can a plane. We can partition the earth's surface into 20 equilateral spherical triangles (a spherical icosahedron); however, this is the limit of equal triangular divisions [*Wenninger,* 1979]. In order to conduct high-resolution studies, we require denser triangular grids on the spherical surface. We present here a simple, approximately uniform spherical-triangular tessellation method based upon the result from plane geometry that the line joining the midpoints of two sides of a given equilateral triangle is parallel to its third side and equal in length to half of it; therefore, the triangle is partitioned into four equilateral sub-triangles. This procedure can be repeated as many times as are desired until the desired resolution is attained. This dyadic subdivision has been applied to the spherical finite-element modeling [*Baumgardner and Frederickson,* 1985]. It is easy to extend the procedure to allow partition of a spherical triangle with either an odd or even integral frequency.

To demonstrate the method, it suffices to consider a single equilateral spherical triangle, by virtue of the

[1]Now at Department of Earth and Planetary Sciences, Harvard University, Cambridge, Massachusetts

Paper number 95GL03080
0094-8534/95/95GL-03080$03.00

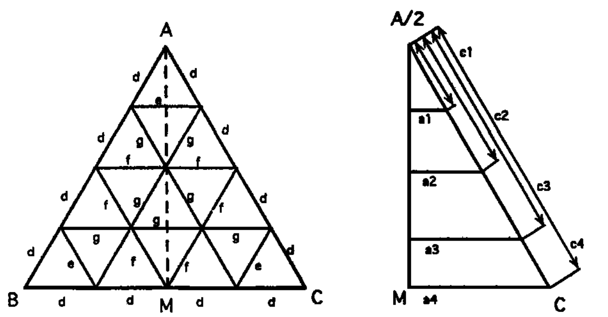

Figure 1. Schematic illustration of the 3-fold tessellation of a spherical icosahedral triangle. *Left*: A 3-fold tessellated triangle ABC. M is the midpoint of side BC. *Right*: Blowup of right spherical triangle AMC in ABC.

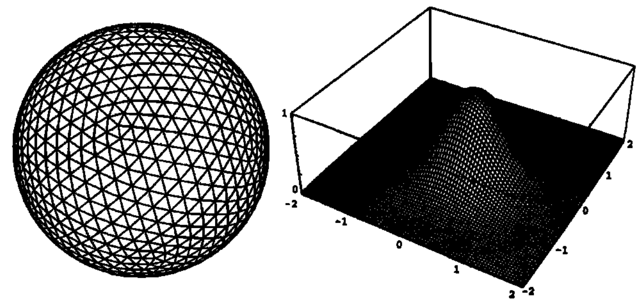

Figure 2. *Left*: Tessellated spherical triangles generated by a 9-fold subdivision of an icosahedron. *Right*: Normalized cubic surface B-spline basis function; each horizontal unit is $\bar{\Delta}$.

symmetric feature of the spherical icosahedron. Fig. 1 shows a 3-fold partition, in which each side is divided into four equal arcs; the flat triangle must be imagined projected onto the surface of a sphere. For the right spherical triangle AMC shown on the right, we have the following relation from spherical trigonometry: $\sin a_i = \sin(A/2)\sin c_i$. The angle A is 72°. The index i varies from 1 to 4. The lengths of the arcs d, e, f, g are given by the following relations: $d = c_1, e = 2a_1, f = a_2, g = 2\,a_3/3$. It is straightforward to extend this 3-fold example to the n-fold case without extra effort.

For an n-fold triangular tessellation, the total number of knots or vertices on the sphere is $N = F/2+2$, where F is the number of triangular faces, given by $F = 20\,(n+1)^2$. Table 1 shows a list of the n-fold tesselations, together with their typical angular side length $\bar{L}$, number of knots N, number of faces F, the nominal degree $\bar{l}$ of the equivalent spherical-harmonic representation, and the number of associated spherical-harmonic coefficients $(\bar{l}+1)^2$. The nominal degree $\bar{l}$ corresponding to each fold level is related to the average side length by $\bar{l} = \mathrm{int}\,(180°/\bar{L})$. The maximum departure of the side lengths away from the average is less than 8%. Fig. 2 (*left*) shows a 2000-triangle tessellation with 1002 knots having an average geodesic separation of approximately 6°. The vertices form a set of nearly uniformly distributed knots on the surface of the sphere.

Table 1. List of folds and associated number of faces, knots, averaged length and percent variation, and the nominal degree of the equivalent spherical-harmonic model (see text for definition)

n	F	N	$\bar{L}$	Var (%)	$\bar{l}$	$(\bar{l}+1)^2$
0	20	12	63.4°	0.0	3	16
1	80	42	31.7°	6.3	6	49
2	180	92	21.1°	7.3	9	100
3	320	162	15.8°	7.6	11	144
4	500	252	12.7°	7.8	14	225
5	720	362	10.6°	7.9	17	324
6	980	492	9.0°	7.9	20	441
7	1280	642	7.9°	7.9	23	576
8	1620	812	7.0°	8.0	26	729
9	2000	1002	6.3°	8.0	29	900

Spline Parameterization

To represent a two-dimensional function of the colatitude θ and longitude ϕ, we define a set of cubic B-spline base functions in terms of the geodesic distance Δ measured from a number of nearly even-distributed knots on the spherical surface, constructed using the method described above. The normalized cubic B-spline function centered upon each knot is given by [*Lancaster and Salkauskas,* 1986]:

$$f = \begin{cases} \frac{3}{4}\bar{\Delta}^{-3}\Delta^3 - \frac{6}{4}\bar{\Delta}^{-2}\Delta^2 + 1, & \Delta \le \bar{\Delta}, \\ -\frac{1}{4}\bar{\Delta}_1^3 + \frac{3}{4}\bar{\Delta}_1^2 - \frac{3}{4}\bar{\Delta}_1 + \frac{1}{4}, & \bar{\Delta} \le \Delta \le 2\bar{\Delta} \end{cases}$$

where $\bar{\Delta}$ is the average angular distance between neighbouring knots, $\Delta_1 = \Delta - \bar{\Delta}$, and $\bar{\Delta}_1 = \Delta_1/\bar{\Delta}$. In fact, the quantity $\bar{\Delta}$ can be varied, e. g. in a regional study with non-uniform coverage. Fig. 2 (*right*) shows a schematic surface plot of this cubic B-spline function. Each local basis function is axially symmetric with respect to its knot; both f and its derivatives vanish for $\Delta \ge 2\bar{\Delta}$. A two-dimensional function such as a surface-wave phase velocity c at any point θ, ϕ on the sphere can be expressed as $c(\theta,\phi) = \sum_{i=1}^{N} f_i(\Delta)a_i$, where a_i is the model coefficient at knot i. Given the value of the local model parameter at each knot, we can obtain the coefficients by solving the linear system of equations $\mathbf{c} = \mathbf{Fa}$, where $c_i = c(\theta_i,\phi_i)$, and $F_{ij} = f_j(\Delta_{ij})$, where Δ_{ij} is the geodesic distance from the ith knot to the jth knot. In an inversion study, the model coefficients at the N knots can be directly determined.

In order to perform kinematic and dynamic surface-wave raytracing using such a local-basis model representation, we need to calculate the first and second derivatives of the phase velocity with respect to θ and ϕ on a spherical surface-spline parameterization. The first-order derivatives are given by

$$\frac{\partial c(\theta,\phi)}{\partial x_j} = \sum_{i=1}^{N} a_i \frac{\partial f_i}{\partial \Delta}\frac{\partial \Delta}{\partial x_j},$$

and the second-order derivatives are expressed in a form

$$\frac{\partial^2 c(\theta,\phi)}{\partial x_j \partial x_k} = \sum_{i=1}^{N} a_i \left(\frac{\partial^2 f_i}{\partial \Delta^2} \frac{\partial \Delta}{\partial x_j} \frac{\partial \Delta}{\partial x_k} + \frac{\partial f_i}{\partial \Delta} \frac{\partial^2 \Delta}{\partial x_j \partial x_k} \right),$$

where $j,k = 1,2$, $x_1 = \theta$ and $x_2 = \phi$. The derivatives $\partial f/\partial\Delta$ and $\partial^2 f/\partial\Delta^2$ can be calculated readily. It is noteworthy that the derivatives of the angular epicentral distance Δ with respect to θ and ϕ are singular at $\Delta = 0$. For the first-order derivatives this singularity is cancelled by $\partial f/\partial\Delta$. It is less obvious how to deal with the singularity of the second derivatives in the limit when $\Delta \to 0$. By using the Taylor expansion at θ_i, ϕ_i and retaining only the terms of first order in $\delta\theta$ and $\delta\phi$, the second-order derivatives of the ith basis function in the vicinity of the ith knot can be given by

$$\begin{aligned}
\frac{\partial^2 f_i}{\partial \theta^2} &= -3\bar{\Delta}^{-2} + \frac{9}{4}\bar{\Delta}^{-3}\left(\delta\Delta + \frac{\delta\theta^2}{\delta\Delta}\right), \\
\frac{\partial^2 f_i}{\partial \phi^2} &= -3\bar{\Delta}^{-2}(s^2 - \frac{s_2\delta\theta}{2}) + \frac{9}{4}\bar{\Delta}^{-3}s^4 s_3, \\
\frac{\partial^2 f_i}{\partial \theta \partial \phi} &= -\frac{3}{2}\bar{\Delta}^{-2}s_2\,\delta\phi + \frac{9}{4}\bar{\Delta}^{-3}s^2\,\frac{\delta\theta\delta\phi}{\delta\Delta}.
\end{aligned}$$

where $s = \sin\theta_i$, $s_2 = \sin 2\theta_i$, $s_3 = \delta\Delta + s^2\delta\phi^2/\delta\Delta$, and $\delta\Delta$, $\delta\theta$ and $\delta\phi$ are the variations in Δ, θ and ϕ in the vicinity of θ_i, ϕ_i.

Synthetic Seismograms

Fig. 3 compares the JWKB phase and amplitude anomalies of 150-second vertical-component R1 Rayleigh waves calculated using the local surface-spline and global spherical-harmonic parameterizations at fifty stations for twenty large earthquake between 1977-1984. A 4-fold tessellation scheme with 252 knots covering the whole earth surface is used in the local surface-spline parameterization; this is equivalent in resolution to a spherical-harmonic model of degree 14. Only paths with epicentral distances in the range $60° < \Delta < 120°$ are considered in this test to avoid the interference of even and odd surface-wave arrivals near the source and antipode. Both the phase and amplitude anomalies of the surface-spline parameterization are in very good agreement with those of the spherical-harmonic representation. The amplitude anomalies are more discrepant than the phase anomalies due to the fact that they depend upon $\nabla\nabla c$, which is represented by locally conical basis functions. Fig. 4 compares the vertical-component waveform of the R1 fundamental-mode Rayleigh waves for two typical raypaths OXA–BJT and NCP–CTAO in the period range 100-300 seconds. The NCP–CTAO path is only slightly deviated from the great circle whereas the OXA–BJT is deflected from the great-circle path by more than 3° (see Fig. 17a of *Wang and Dahlen* [1994]). In both cases the waveforms are essentially indistinguishable. The corresponding spectra shown in Fig. 5 reveal small errors in amplitude due to the local conical representation of $\nabla\nabla c$.

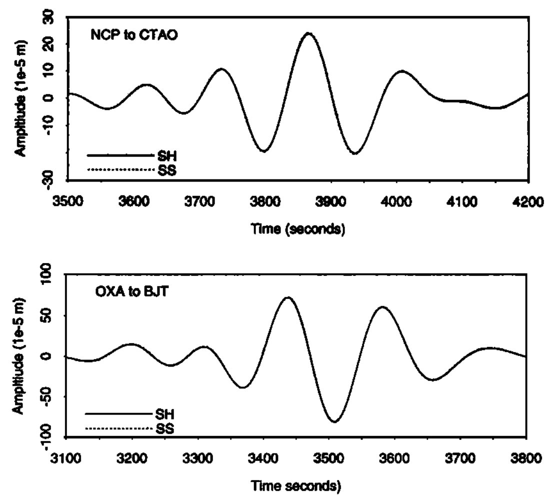

Figure 4. JWKB waveforms calculated using the spherical surface-spline (SS: dashed line) and spherical-harmonic (SH: solid line) representations. *Top:* Path from near the Coast of Peru (NCP) to CTAO. *Bottom:* Path from Oaxaca, Mexico (OXA) to BJT.

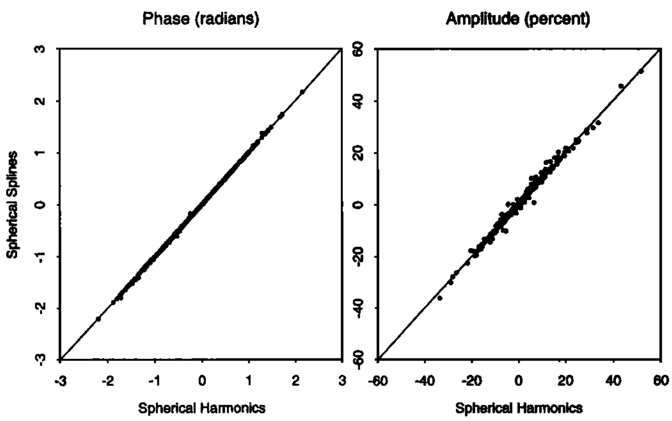

Figure 3. JWKB phase anomalies $\psi - \psi_{\rm sph}$ and fractional amplitude anomalies $(A - A_{\rm sph})/A_{\rm sph}$ of 150-second vertical-component R1 Rayleigh waves calculated using a spherical surface-spline and a spherical-harmonic representation for 506 paths. Each dot represents one path.

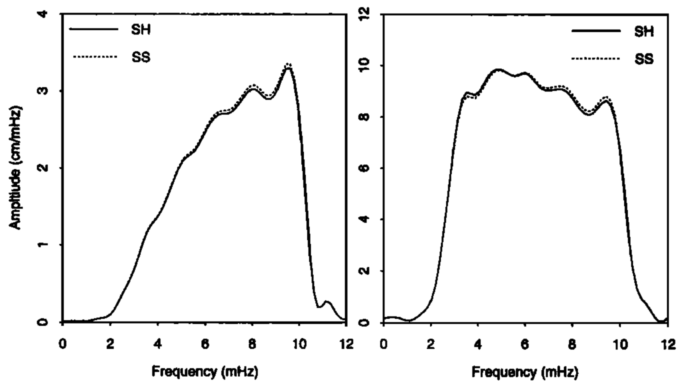

Figure 5. Amplitude spectra corresponding to the synthetic spectra of the seismograms in Fig. 4.

Table 2. Comparison of CPU time (Minutes) needed to calculate inversion kernels for 1560 paths on a Sparc 20.

Model	S12_WM13	Degree 36
Spherical Harmonics	70	872
Surface Splines	40	43

Conclusion

A spherical tessellation method is used to partition the earth's surface into a set of approximately equilateral spherical triangles, whose vertices or knots have approximately the same nearest-neighbor separation. Based upon this knot system, a spherical cubic B-spline method is developed to parameterize a two-dimensional function on a sphere. Such a parameterization can represent a global function with the same accuracy as the spherical-harmonic representation at the equivalent resolution on the one hand, and be applied to regional inversion studies due to the local character of the basis functions on the other hand. Unlike the spherical-harmonic representation, the spherical surface-spline model is expanded in terms of a set of locally defined basis functions centered upon the grid of knots. To evaluate the model at a given point on the sphere, we only need to account for the contribution from the knots situated within two inter-knot arclengths of the target point, regardless of the fold level. This allows us to increase the resolution of the model without additional computation time in calculating surface-wave inversion kernels.

The practicality of applying JWKB theory to surface wave phase-velocity inversion relies on a fast forward method of generating the inversion kernel. Most CPU time is consumed in evaluating the phase velocity while performing the two-point raytracing to find the raypath from source to receiver. On a spherical-harmonic model we need to sum $(l+1)^2$ coefficients for each phase-velocity evaluation, whereas with a local spline basis there are approximately 20 neighboring knots involved regardless of the tessellation frequency. A comparison of the CPU time needed to calculate the inversion kernels for 1560 paths on model S12_WM13 and a "roughened" degree-36 model is given in Table 2. It takes approximately 10 times more CPU time for the degree-36 model than for the degree-12 model using a spherical-harmonic representation, whereas the CPU time for the surface-spline model at a resolution equivalent to degree 36 increases only slightly from the surface-spline model equivalent to degree 12.

Acknowledgments. We thank Gabi Laski and two anonymous reviewers for their constructive reviews. This work has been supported by the U. S. National Science Foundation under grant EAR-9117699.

References

Baumgardner, R. B. and P. O. Frederickson, Icosahedral discretization of the two-sphere. *SIAM J. Numer. Anal.* , **22**, 1107–1115, 1985.

Clayton, R. W. and R. P. Comer, A tomographic analysis of mantle heterogeneities from body wave travel time data (abstract). *EOS Trans. AGU*, **64**, 776, 1983.

Constable, C. G., R. L. Parker and P. B. Stark, Geomagnetic field models incorporating frozen-flux constraints, *Geophys. J. Int.*,, **113**, 419–433, 1993.

Lancaster, P. and K. Salkauskas, *Curve and Surface Fitting, an Introduction*, 280 pp., Academic, New York, 1986.

Masters, G., T. H. Jordan, P. G. Silver, and F. Gilbert, Aspherical Earth structure from fundamental spheroidal mode data, *Nature*, **298**, 609–613, 1982.

Su, W., R. L. Woodward, and A. M. Dziewonski, Degree 12 model of shear velocity heterogeneity in the mantle, *J. Geophys. Res.*, **99**, 6945–6980, 1994.

Tromp, J. and F. A. Dahlen, Variational principles for surface-wave propagation on a laterally heterogeneous Earth 2. Frequency-domain JWKB theory, *Geophys. J. Int.*, **109**, 599–619, 1992.

Um, J. and F. A. Dahlen, Source phase and amplitude anomalies of long-period surface waves, *Geophys. Res. Lett.*, **19**, 1575–1578, 1992.

Wang, Z. and F. A. Dahlen, JWKB Surface Wave Seismograms on a laterally heterogeneous Earth, *Geophys. J. Int.*,, **119**, 381–401, 1994.

Wenninger, M. J., *Spherical Models*, 147 pp., Cambridge University Press, Cambridge, England, 1979.

Woodhouse, J. H. and A. M. Dziewonski, Mapping the upper mantle: Three-dimensional modeling of earth structure by inversion of seismic waveforms, *J. Geophys. R.*, **89**, 5953–5986, 1984.

Woodhouse, J. H. and Y. K. Wong, Amplitude, phase and path anomalies of mantle waves, *Geophys. J. R. astr. Soc.*, **87**, 753–773, 1986.

Zhang, Y.-S. and T. Tanimoto, High-resolution global upper mantle structure and plate tectonics, *J. Geophys. R.*, **98**, 9793–9823, 1992.

Z. Wang Department of Earth and Planetary Sciences, Harvard University, Cambridge, Massachusetts 02138 [e-mail: wang@geophysics.harvard.edu]

F.A. Dahlen, Department of Geological and Geophysical Sciences, Princeton University, Princeton, New Jersey 08544 [e-mail: tony@geo.princeton.edu]

(received June 29, 1995; accepted August 14, 1995.)